



Magnetic and Electrical Properties of Nanocrystalline $\text{Fe}_{85}\text{Si}_{10}\text{Ni}_5$ /Phenolic Resin Soft Magnetic Composites

Farzin Mohseni¹, Hamid Reza Madaah Hosseini^{*,1}, Hooman Shokrollahi², Tayebeh Gheiratmand¹

¹Materials Science and Engineering Department, Sharif University of Technology, Tehran, Iran.

²Electrocermics Group, Department of Materials Science and Engineering, Shiraz University of Technology, Shiraz, Iran.

Received: 6 May 2020; Accepted: 20 June 2020

* Corresponding author email: madaah@sharif.edu

ABSTRACT

In this work, nanocrystalline $\text{Fe}_{85}\text{Si}_{10}\text{Ni}_5$ soft magnetic powders were prepared by mechanical alloying and subsequent annealing to reduce the internal stresses and lattice strains. The powders were mixed with phenolic resin and warm pressed to produce nanostructured soft magnetic composites. The effect of annealing time and temperature on the crystalline structure, microstructure and magnetic properties of the powders and composite samples were investigated by XRD, SEM, VSM and LCR techniques. The results show that the annealing causes a significant improvement in the soft magnetic properties of the powders. By increasing the pressure and temperature in the compaction process, the density and permeability of the bulk samples increased. Moreover, increasing the phenolic resin content from 0.8 to 1.2 wt. % improves the electrical resistivity of the nanostructured soft magnetic composites.

Keywords: Soft Magnetic Composite, Nanocrystalline Fe-Si-Ni alloys, Mechanical Alloying, Magnetic Properties

1. Introduction

Soft magnetic materials play an important role in power generation and conversion. They are used in many heavy applications such as transformers and generators. As the energy consumption in the 21st century is booming, the need for high performance and efficient soft and hard magnetic materials is rising. Soft magnetic materials are produced in many forms such as soft iron, silicon steels, soft ferrites and nanocrystalline or amorphous metal alloys [1].

Recently, the number of investigations performed on the nanocrystalline soft magnetic alloys has significantly increased. Among different types of soft magnetic alloys, the nanostructured Fe-Si based alloying systems are most attractive due to their excellent soft magnetic properties [2].

On one hand, the addition of Si into Fe enhances the electrical resistivity and therefore, reduces the eddy current losses. Si reduces the magnetocrystalline anisotropy and coercivity (H_c) of α -Fe crystalline structure [4, 5]. On the other hand, the permeability and electrical resistivity increase by adding Ni to Fe [3]. Our previous studies on Fe-Si-Ni systems have demonstrated that the optimum composition for high saturation magnetization and low coercivity belongs to $\text{Fe}_{85}\text{Si}_{10}\text{Ni}_5$ soft magnetic alloy [3, 6].

Soft Magnetic Composites (SMCs) are basically soft magnetic powder particles isolated by a very thin electrically insulating layer. Efficient insulation of fine particles generally leads to the reduction in eddy current losses at high-frequency applications. At low frequencies, insulation is less critical but needed to minimize the negative effect of the eddy

currents on the magnetization of the material [7]. The physical and mechanical properties of phenolic resin make it a good candidate as an insulation layer which has been investigated in many studies [8-11].

SMCs could be applied in a wide range of applications from electromagnetic interference filters, smoothing chokes in switch mode power supplies, radiofrequency coupling devices, to radiofrequency tuning cores and filter inductors, converters, transformers, electrical micromotors and low power motors for automation and robotics [12, 13].

In this study, the pure elemental Fe, Si and Ni powders were milled to form mechanically alloyed (MA) $\text{Fe}_{85}\text{Si}_{10}\text{Ni}_5$ powders. The MA powders were then annealed, mixed with phenolic resin and compressed by a warm compaction process. The effects of annealing treatment, compaction parameters and resin content on the structure, magnetic and electrical properties were investigated.

2. Experimental Procedure

2.1. Powder preparation

The elemental Fe, Si and Ni powders with ~99.5 wt. % purity were used as the starting materials to produce an alloy with a nominal composition of $\text{Fe}_{85}\text{Si}_{10}\text{Ni}_5$ at.%. The mixed powders were milled under argon atmosphere in a high-energy vibratory mill with a ball to powder weight ratio (BPR) of 15:1 at the rotation speed of 750 rpm for 180 min. To decrease the internal strains, annealing was performed at different temperatures of 500, 550 and 600 °C under argon atmosphere for 1 h. Table 1 shows the annealing conditions of the powders in each series of powder samples.

2.2. NSMC's Samples preparation

In order to prepare bulk NSMC sample, the prepared single phased nanostructured $\text{Fe}_{85}\text{Si}_{10}\text{Ni}_5$ (at. %) powders were mixed with 0.8 and 1.2 wt. % of a thermoset phenolic resin. The mixture was then shaken in a Turbula-2TC shaker for 30 minutes to obtain a homogenous mixture. The bulk samples were prepared by warm compressing the

Table 1- The annealing conditions of the powders for each series of the powder samples

Series Number	Annealing Condition
1	Not Annealed
2	500 °C/ 1h/ Argon
3	550 °C/ 1h/ Argon
4	600 °C/ 1h/ Argon

mixture in a 16 mm diameter cylindrical die under a compressive pressure of 400, 600, 800 and 1000 MPa at 70 °C. For comparing the effect of warm compaction on the bulk samples, a series of samples were prepared by cold pressing under 400, 600, 800 and 1000 MPa pressure. In order to cure the resin, samples were then heated at 170 °C for 1 h in air.

2.3. Characterization

The morphology of the particles and bulk samples was characterized by a VEGA- TESCAN scanning electron microscope (SEM). The crystal structural characterization was performed with Cu K α radiation ($\lambda=1.5406 \text{ \AA}$) using X'Pert Pro MPD-XRD X-ray Diffraction (XRD) instrument. The full-width half maximum (FWHM) values of the XRD peaks were estimated using the X'pert software. The crystallite size and lattice strain were calculated using the following equation via the Williamson-Hall method [14]:

$$\beta_s \cos\theta = \frac{k\lambda}{d} + 2\epsilon \sin\theta \quad (1)$$

Where β_s is the FWHM of the diffraction peak, θ is the Bragg angle, ϵ is the internal micro-strain, and d is the crystallite size. β_s can be derived from:

$$\beta_{s-\text{Actual}} = \sqrt{\beta_m^2 - \beta_{ins}^2} \quad (2)$$

Where β_{ins} is the width at half-maximum of the Si powder peaks used for calibration and β_m is the evaluated width.

The magnetic properties including saturation magnetization (M_s), hysteresis loss and coercive force (H_c) were measured using a Vibrating Sample Magnetometer (VSM) at room temperature with a maximum field of 10 kOe and instrumental error of 2%. Frequency dependent magnetic properties of the bulk samples were characterized using an Inductance Capacitance Resistance (LCR) meter. The density of the bulk samples was measured by the Archimedean method.

3. Results and Discussion

3.1. Powder samples

Fig. 1 illustrates the XRD pattern of the milled $\text{Fe}_{85}\text{Si}_{10}\text{Ni}_5$ powder for 180 min. The XRD pattern confirms that all the diffraction peaks match with ana-Fe solid solution, which confirms the formation of a single phased alloy after 180 min of milling. As shown in Figs. 2 and 3, by increasing the annealing temperature of the mechanically alloyed

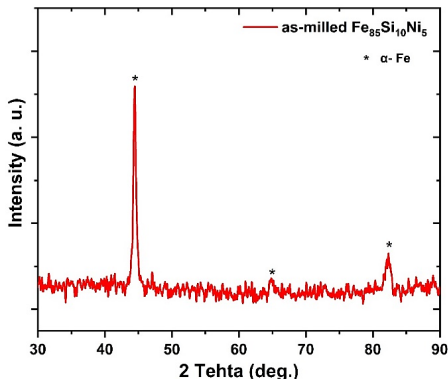


Fig. 1- XRD pattern of the as-milled $\text{Fe}_{85}\text{Si}_{10}\text{Ni}_5$ powders after 180 min of milling.

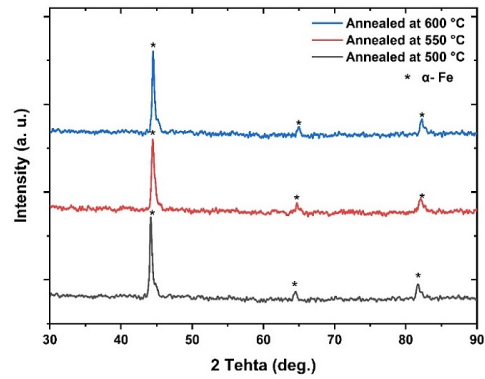


Fig. 2- XRD pattern of $\text{Fe}_{85}\text{Si}_{10}\text{Ni}_5$ powder annealed at 500, 550 and 600 °C.

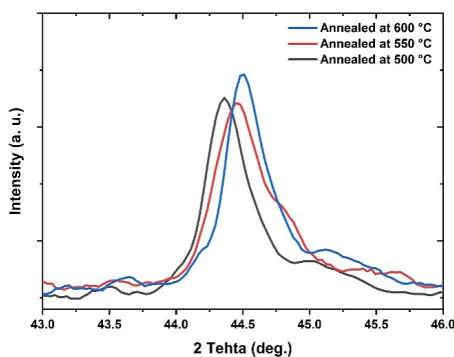


Fig. 3- The shift in the main peak of the XRD pattern for $\text{Fe}_{85}\text{Si}_{10}\text{Ni}_5$ powders annealed at 500, 550 and 600 °C.

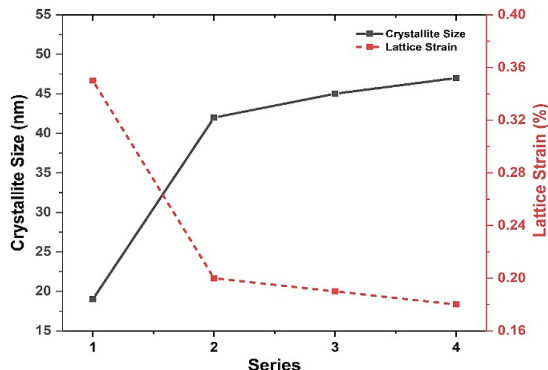


Fig. 4- Crystallite size and lattice strain of the powder samples before and after annealing at different temperatures.

powders, the peaks are sharpened and shifted slightly to the right. The reduction in the width of the peaks could be due to the increase in the crystallite size of powders by annealing at higher temperatures which also decreases the residual compressive internal micro-strains in the powders. This reduction could cause a shift in the XRD patterns to higher 2 theta angles. Fig. 4 shows the effect of annealing treatment on the internal micro-strains and the crystallite size of the powders. It can be seen that by annealing the as-milled powders at 500 °C for 1 h, the crystallite size increases from ~ 20 nm to 45 nm and the micro-strain decreases from ~ 0.36 % to ~ 0.2 %. This increase in the crystallite size and micro-strain reduction continues with increasing the annealing temperature up to 600 °C with a smaller rate.

Although the crystallite size increases by annealing the as-milled powders, the SEM images of the as-milled and annealed at 600 °C $\text{Fe}_{85}\text{Si}_{10}\text{Ni}_5$ powders show no significant changes in the morphology and particle size of the powder samples (Fig 5).

Table 2 shows the room temperature saturation magnetization (M_s), coercivity (H_c) and the hysteresis loss of the powder samples before and after annealing at different temperatures. By increasing the annealing temperatures, the H_c of the powder samples decreases. The crystalline defects prevent the ease of the domain wall movement as well as the domain rotation, which subsequently increase the magnetic H_c . As the annealing temperature increases, the amount of lattice defects such as dislocations and micro-strains decreases. Even though the magnetic measurements show a slight decrease in the M_s of the annealed powders compared to the as-milled $\text{Fe}_{85}\text{Si}_{10}\text{Ni}_5$, the decrease in the H_c leads to a decrease in the hysteresis loss which subsequently leads to an improvement in the soft magnetic properties of the annealed powders compared to the as-milled $\text{Fe}_{85}\text{Si}_{10}\text{Ni}_5$.

3.2. Bulk NSMC samples

In order to investigate the effects of various compaction conditions on the density, morphology,

Table 2- Room temperature magnetic properties of the mechanically alloyed $\text{Fe}_{85}\text{Si}_{10}\text{Ni}_5$ powders before and after annealing at different temperatures

Annealing Temperature (°C)	Not Annealed	500	550	600
Saturation Magnetization (emu/g)	182	178	178	178
Coercivity (Oe)	59	55	53	52
Hysteresis Loss (kOe.emu/g)	79.9	75.3	71.4	69.7

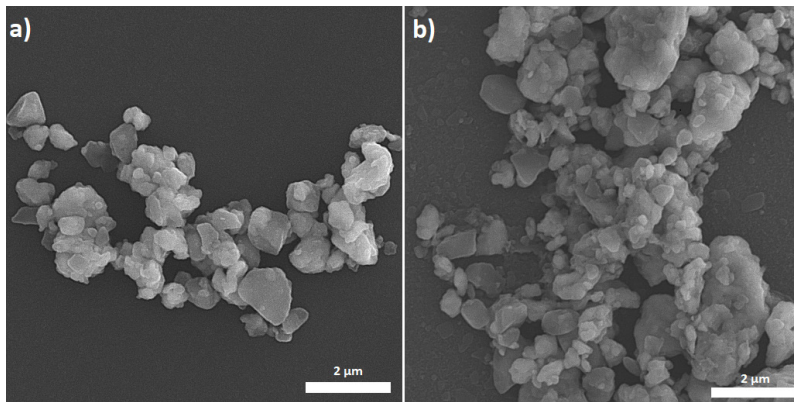


Fig. 5- SEM micrograph of (a) as-milled $\text{Fe}_{85}\text{Si}_{10}\text{Ni}_5$ powders for 180 min and (b) annealed for 1 h at 600 °C.

electrical and magnetic properties of compressed $\text{Fe}_{85}\text{Si}_{10}\text{Ni}_5$, bulk samples were prepared by a warm compaction process and a cold press followed by curing. Fig. 6 shows the rise in the compaction pressure leads to an increase in the density of the composite samples. However, at higher pressures, the increase in the density occurs at a slower slope and it maximized in the sample warm pressed at 1000 MPa. This may be due to the intense plastic deformation of powders at higher pressures. This effect had been reported in other researches [15]. In addition, warm compaction leads to the larger values of density compared to the cold pressed and cold pressed then cured samples. In the warm compaction process, the ease of powder rearrangement and movement in the phenolic resin matrix and the ease of plastic deformation cause higher density at the same pressure. The observed maximum density of the bulk samples is ~ 6.7 g/cc which is ~ 95% of the theoretical density (~ 7.03 g/cc) of the pure $\text{Fe}_{85}\text{Si}_{10}\text{Ni}_5$ alloy.

In order to compare the morphology of the warm compressed sample with the cold pressed followed by a curing process, SEM was applied (Fig. 7). The post heating process on the cold pressed samples causes the curing of the resin which ultimately causes an increase in the density of the bulk samples. However, during the warm compaction process, the particle rearrangement causes a more

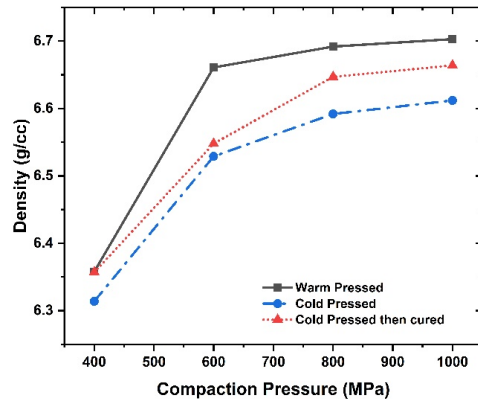


Fig. 6- The effect of the compaction pressure on the density of $\text{Fe}_{85}\text{Si}_{10}\text{Ni}_5$ SMC's with 0.8 wt.% Phenolic resin.

uniform densification which ultimately leads to a lower amount of porosities and higher densities.

Fig. 8 shows the electrical resistivity measurements on the bulk samples. The increase in the compaction pressure, in both cold pressed and warm pressed samples causes a small rise in the electrical resistivity. In high pressures, the phenolic resin covers the soft magnetic particles more uniformly which leads to an increase in the electrical resistivity of the samples. The post heating treatment significantly increases the electrical resistivity due to the curing of the resin. An increase in the phenolic resin content from 0.8 wt. % to 1.2

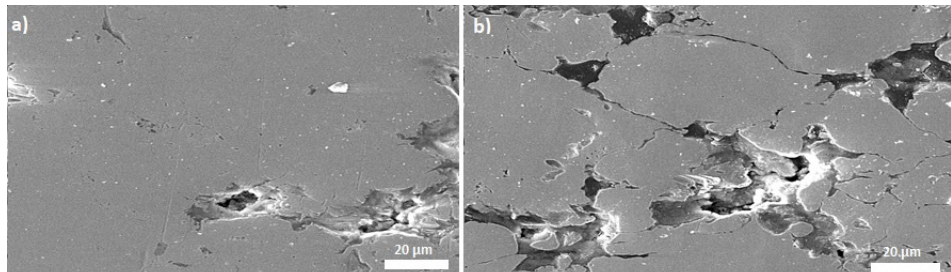


Fig. 7- SEM image of the composite sample (a) warm compacted under 800 MPa at 70°C and (b) cold pressed then cured at 170 °C for 1 h.

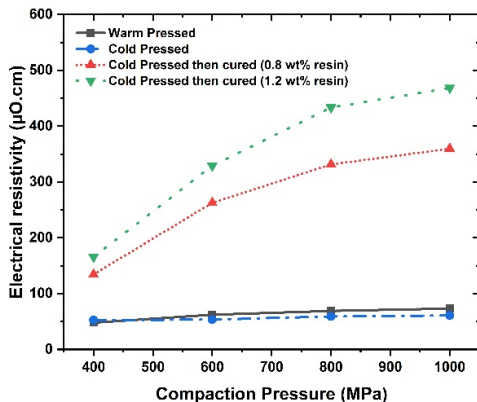


Fig. 8- The effect of compaction pressure on the electrical resistivity of the $\text{Fe}_{85}\text{Si}_{10}\text{Ni}_5$ SMC's with 0.8 wt.% and 1.2 wt.% Phenolic resin.

wt. % further increases the electrical resistivity, due to the thickening of the resistive layer between the soft magnetic powders.

Fig. 9 shows variation of permeability with compaction pressure of the warm pressed samples. The permeability increases by enhancing the compaction pressure. As the compaction pressure increases, the density increases, and the amount of porosities decreases. The more magnetic mass exists per equal volume results in the increase of permeability. This result is in agreement with what has been reported in the literatures [11, 15]. As the frequency rises, the eddy current loss increases and consequently, the permeability declines. It is well known that density and residual stresses affect the permeability directly. The contrast between these two parameters causes a reduction in the amount of increase in the permeability in pressures higher than 600 MPa.

Fig. 10 illustrates the effect of resin content on the permeability of the bulk samples at different frequencies. Increasing the resin content in NSMC samples from 0.8 wt.% to 1.2 wt. % causes a slight increase in the relative density due to the better

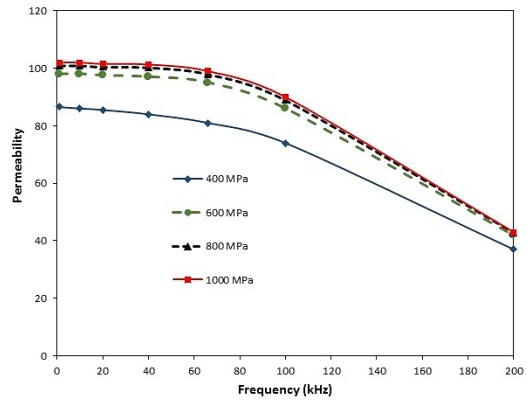


Fig. 9- Variation of permeability as a function of frequency for the composite samples compacted at different pressures.

coating and subsequently connecting the particles, and it also reduces the residual stresses in the samples owing to the exposing to higher temperatures which leads to an increase in the permeability of the samples. The curing treatment on the compressed samples removes most of the residual stresses and causes a significant increase in the permeability of the composite samples (Fig. 11).

4. Conclusions

A high-energy vibratory mill was used to prepare nanostructured soft magnetic $\text{Fe}_{85}\text{Si}_{10}\text{Ni}_5$ alloy powders with an average crystallite size of ~ 19 nm. It was shown that the annealing treatment can eliminate the residual stresses which have a pinning effect on domain rotation and domain wall movement. The lattice strain and magnetic coercivity decrease by increasing the annealing temperature. While the annealing process of the powders causes a slight decrease in the M_s of the powder samples, the optimized soft magnetic properties occur in the powder sample annealed at 600°C, with the least H_c and hysteresis loss. Bulk NSMC samples were prepared by mixing the optimized

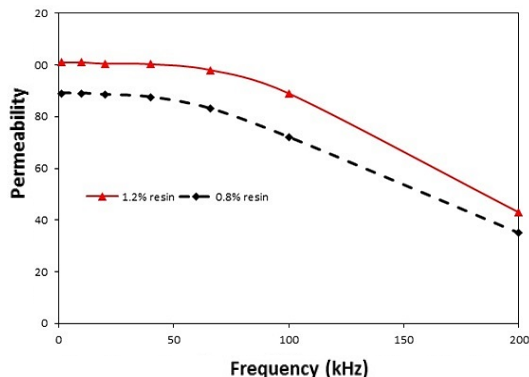


Fig. 10- Permeability as a function of frequency for the composite samples with different resin contents

soft magnetic powders with various amounts of phenolic resin followed by a warm compaction and cold compaction process. The results show that increasing the compaction pressure and applying a warm compaction process improves the density of the samples. Post heating treatment was performed

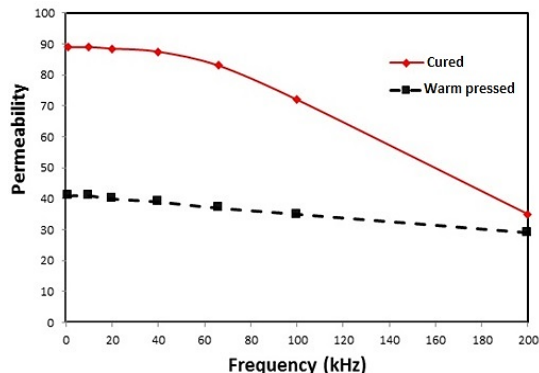


Fig. 11- The effect of curing treatment on the permeability of composite samples.

on the bulk samples to cure the phenolic resin, which leads to a significant increase in the electrical resistivity, as well as the permeability of the NSMC's. We also observed that increasing the phenolic resin content from 0.8 to 1.2 wt.% enhances both the permeability and electrical resistivity.

References

- Gutfleisch O, Willard MA, Brück E, Chen CH, Sankar SG, Liu JP. Magnetic Materials and Devices for the 21st Century: Stronger, Lighter, and More Energy Efficient. *Advanced Materials*. 2010;23(7):821-42.
- Gheiratmand T, Hosseini HRM. Finemet nanocrystalline soft magnetic alloy: Investigation of glass forming ability, crystallization mechanism, production techniques, magnetic softness and the effect of replacing the main constituents by other elements. *Journal of Magnetism and Magnetic Materials*. 2016;408:177-92.
- Madaah Hosseini HR, Bahrami A. Preparation of nanocrystalline Fe-Si-Ni soft magnetic powders by mechanical alloying. *Materials Science and Engineering: B*. 2005;123(1):74-9.
- Ding J, Li Y, Chen LF, Deng CR, Shi Y, Chow YS, et al. Microstructure and soft magnetic properties of nanocrystalline Fe-Si powders. *Journal of Alloys and Compounds*. 2001;314(1-2):262-7.
- Števulová N, Buchal A, Petrovič P, Tkáčová K, Šepelák V. Structural investigation of the high-energy milled Fe-Si system. *Journal of Magnetism and Magnetic Materials*. 1999;203(1-3):190-2.
- Bahrami A, Madaah Hosseini HR, Abachi P, Miraghaei S. Structural and soft magnetic properties of nanocrystalline Fe85Si10Ni5 powders prepared by mechanical alloying. *Materials Letters*. 2006;60(8):1068-70.
- Shokrollahi H, Janghorban K. Soft magnetic composite materials (SMCs). *Journal of Materials Processing Technology*. 2007;189(1-3):1-12.
- Taghvaei AH, Shokrollahi H, Janghorban K. Magnetic and structural properties of iron phosphate-phenolic soft magnetic composites. *Journal of Magnetism and Magnetic Materials*. 2009;321(23):3926-32.
- Dias MM, Mozetic HJ, Barboza JS, Martins RM, Pelegri L, Schaeffer L. Influence of resin type and content on electrical and magnetic properties of soft magnetic composites (SMCs). *Powder Technology*. 2013;237:213-20.
- Taghvaei AH, Shokrollahi H, Ebrahimi A, Janghorban K. Soft magnetic composites of iron-phenolic and the influence of silane coupling agent on the magnetic properties. *Materials Chemistry and Physics*. 2009;116(1):247-53.
- Taghvaei AH, Shokrollahi H, Ghaffari M, Janghorban K. Influence of particle size and compaction pressure on the magnetic properties of iron-phenolic soft magnetic composites. *Journal of Physics and Chemistry of Solids*. 2010;71(1):7-11.
- Gramatyka P, Nowosielski R, Sakiewicz P. Magnetic properties of polymer bonded nanocrystalline powder. *Journal of Achievements in Materials and Manufacturing Engineering*. 2007 Jan;20(1-2):115-8.
- Maeda T, Toyoda H, Igarashi N, Hirose K, Mimura K, Nishioka T, Ikegaya A. Development of super low iron-loss P/M soft magnetic material. *SEI TECHNICAL REVIEW*. 2005 Jun;60:3-9.
- Williamson GK, Hall WH. X-ray line broadening from filed aluminium and wolfram. *Acta Metallurgica*. 1953;1(1):22-31.
- Gheiratmand T, Madaah Hosseini HR, Seyed Reihani SM. Iron-borosilicate soft magnetic composites: The correlation between processing parameters and magnetic properties for high frequency applications. *Journal of Magnetism and Magnetic Materials*. 2017;429:241-50.